Analysis of OBS and MCS data offshore Oregon: Estimation of elastic properties of gas hydrates

Mrinal K. Sen*, Chengshu Wang, and Nathan L. Bangs, The University of Texas at Austin

Abstract

The inversion of seismic data offers a tool for the remote extraction of physical properties of the sediments from surface-recorded data. Physical properties of the gas hydrate-bearing sediments derived from inversion of seismic help us identify the presence of gas hydrates. They can also be used to study their character, formation and distribution, and to estimate the amount of gas hydrate and/or free gas that may be present in the sediments. A 3-D multi-channel seismic (MCS) and ocean bottom seismometer (OBS) survey in the Hydrate Ridge, offshore Oregon was conducted to image structures controlling the migration of methane-rich fluid and free gas and to map the gas-hydrate distribution. We first obatined preliminary V_p and V_s profiles from OBS data by interactive analysis and then used them as a starting model to estimate V_p from the streamer data by waveform inversion. The results from our inversion and interpretation study in Hydrate Ridge reveal that: (1) both 3-D streamer and OBS data show a strong BSR indicating the presence of gas hydrate above and free gas below; (2) interactive P- and S-wave velocity analysis of OBS data allows us to identify the presence of a "conversion surface" in the gas hydrate-bearing sediments; (3) inverted velocity profiles show a low-velocity layer existing below the sea floor and above the normal gas hydrate, suggesting a new geological model of gas hydrates; (4) two types of hydrate fabrics, massive and porous hydrates, observed by deep-towed video survey, were identified in the P-wave velocity profiles, and three main layers of gas hydrate-sediments separated by the conversion surface and BSR are distinguished; (5) the profiles reflecting the physical properties of sediments, such as the P-wave velocity, acoustic impedance and Poisson's ratio profiles, are able to map the distribution of gas hydrates and show very similar trends of lateral variation of the main layers; (6) a series of faults in the accretionary complex under the ridge not only offer pathways for methane and fluid ascending from deeper layers but also control the distribution of the porous hydrates with low velocity below the seafloor, and (7) Hornbach et al. (2003) suggest their results using velocity analysis of seismic reflection data on the Blake Ridge is the first direct seismic detection of concentrated hydrate confirmed by velocity analysis. Our results of direct inversion of seismic data extend these results to greater resolution of the entire seismic data set. Further, our results may be the first seismic indication of visually observed porous hydrate zone.

Introduction

Gas hydrates, ice-like crystalline substances are composed of water and gas in which a solid-water lattice accommodates guest gas molecules (largely methane) in a cage-like structure (Sloan, 1990). The gas hydrates have recently become a major focus of international research. The formation and occurrence of natural gas hydrates, found in marine, permafrost, and lake environments worldwide, need appropriate thermodynamic stability conditions for methane-hydrate (Kvenvolden, 1988, 1993; Sloan, 1998; Buffett, 2000) and adequate supplies of gas (mainly methane) and water (Collett, 2002). Gas hydrates are important primarily because they may store large amounts of methane, and secondarily because they influence the physical properties of the gas hydrate-bearing sediments masking images of deeper structure. On seismic sections from continental margins, gas hydrates can be detected mainly by the occurrence of a bottom-simulating reflector (BSR), which, with a negative polarity, is believed to represent the base of the gas hydrate stability zone, marking the transition between hydrate-bearing sediments above and the presence of free gas or water below the surface, and mimicking the relief of the sea floor (Stoll and Bryan, 1978; Shipley et al., 1979; Kvenvolden and Barnard, 1983, Hyndman and Spence, 1992). This lower boundary of solid gas hydrates is present from ~100 to 1100 m below sea floor (Kvenvolden, 1993).

The continental slope of the Oregon accretionary margin, the southern part of the Cascadia accretionary margin, is one of the areas of comprehensive studies of submarine gas hydrates in the world. Based on the observation on 1989 multi-channel seismic data that a BSR is ubiquitous beneath the Hydrate Ridge and the evidence for hydrate and free gas that was found in the same area, a new seismic survey comprising 3-D multi-channel seismic (MCS) streamer and Ocean Bottom seismometers (OBS) surveys, aimed at imaging the structures controlling the migration of methane-rich fluid and free gas and characterizing the gas hydrates of the southern part of the Hydrate Ridge, was conducted in the Summer of 2000 (Fig. 1). The objectives of our research include: (1) Velocity analysis of Vp and Vs from OBS data, (2) Pre-stack waveform inversion for Vp in τ-p domain from streamer data, (3) Detection of the distribution of gas hydrates and free gas, and (4) Interpretation of the formation of gas hydrates.

In this paper we report on the results from analysis of some of the seismic data sets obtained from the Oregon seismic experiment. In particular, we derive estimates of *in-situ* elastic properties of gas hydrates and define the distribution of gas hydrates under the southern summit of the Hydrate Ridge using ocean-bottom seismometers (OBS) and multi-channel seismic (MCS) data.

Method

The estimation of physical properties of the gas hydrate-bearing sediments from seismic data allows us to identify the presence of gas hydrates, to study their character, formation and distribution, and to estimate the amount of gas hydrate and/or free gas that may be present in the sediments. The inversion of seismic data offers a tool for remote extraction of physical properties of the sediments from surface-recorded data.

In our research, OBS and MCS data obtained from the central Oregon continental margin experiment are combined to identify main reflecting horizons and estimate physical properties of individual layers, including the character of the hydrates. In general, MCS data can provide the images of the sub-sea structure, and P-wave velocity files; and OBS data can be used to derive high-resolution P-wave and S-wave velocity profiles at sparse locations.

The use of both P- and S-wave reflections in the OBS data can help in robust estimates of P- and S-wave velocities. After the necessary plane wave processing of the OBS data, the interactive P- and S-wave velocity analysis in τ-p domain is used to estimate P- and S-wave velocities. P-wave rms (root mean square) velocity can be routinely obtained from normal moveout of hydrophone common mid-point (CMP) gathers. However, the procedure for estimation of S-wave velocity from P-SV reflection is slightly different. The general procedure for obtaining the estimate of S-wave velocity inlcudes:

- Estimate the Vp/Vs ratio γ from normal incidence PP and PS times.
- Use γ to compute conversion points and sort CMP PS gathers into common coversion point (CCP) gathers.
- Apply an rms stacking velocity analysis (with non-hyperbolic terms) of CCP gathers.

Here we employ τ-p interactive PS velocity analysis of common receiver gathers along strike line (nearly 1D structure) to obtain Vs interval velocity. The τ-*p* trajectory of the PP-waves and the converted PS-waves are given respectively by:

$$\tau_{pp}(p) = 2\, q_p \Delta z, \quad (1)$$

$$\tau_{ps}(p) = \Delta z\, (q_p + q_s), \quad (2)$$

where Δz is the layer thickness, and q_p and q_s the vertical slownesses of the P- and S-waves respectively. For an isotropic medium, we have:

$$\tau_{pp}(p) = 2\tau_p^0 (1 - p^2 v_p^2)^{1/2}, \quad (3)$$

$$\tau_{ps}(p) = \tau_p^0 (1 - p^2 v_p^2)^{1/2} + \tau_s^0 (1 - p^2 v_s^2)^{1/2}, \quad (4)$$

where equation 3 is for PP-wave, and equation 4 is for converted PS-wave and τ_p^0 and τ_s^0 are one-way vertical (zero offset) delay times for P- and S-waves respectively.

The radial component geophone is designed to record S-wave particle motion. In OBS case, the incident wave is P-wave, and the converted waves arriving at the receiving station may be generated in two ways: (1) down-going P-wave is converted into up-going S-wave being reflected at a reflector (denoted as Rps), and (2) down-going P-wave is converted into down-going S-wave during transmission at a conversion surface and then is reflected as up-going S-wave at a lower reflector (denoted as Rpss). For the Rps case, suppose there are n layers of isotropic media, then we have cummulative (total) τ:

$$\tau_{ps}(p) = \sum_{i=1}^{n} \Delta z_i (q_{pi} + q_{si}) \quad (5)$$

$$= \sum_{i=1}^{n} [\tau_{pi}^0 (1 - p^2 v_{pi}^2)^{1/2} + \tau_{si}^0 (1 - p^2 v_{si}^2)^{1/2}],$$

where Δz_i is the *i*th layer thickness, q_{pi} and q_{si} the vertical slownesses of the P- and S-waves for *i*th layer respectively, τ_{pi}^0 and τ_{si}^0 are the one-way delay time for *i*th layer for P- and S-wave at p = 0 respectively, and V_{pi} and V_{si} the velocities of the P-wave and S-wave for *i*th layer respectively. For the Rpss case, suppose that there are n layers of isotropic media and conversion takes place at the reflector between *k*th and (*k*+1)th layers, then we have cumulative (total) τ:

$$\tau_{pss}(p) = \sum_{i=1}^{k} \Delta z_i (q_{pi} + q_{si}) + \sum_{i=k}^{n} 2 q_{si} \Delta z_i \quad (6)$$

$$= \sum_{i=1}^{k} [\tau_{pi}^0 (1 - p^2 v_{pi}^2)^{1/2} + \tau_{si}^0 (1 - p^2 v_{si}^2)^{1/2}] + \sum_{i=k}^{n} 2\tau_{si}^0 (1 - p^2 v_{si}^2)^{1/2}.$$

We estimate P and S wave velocities in the τ-p domain by interactively fitting trajectories for different trial V_p and V_s reflections and examining the NMO corrected data.

To obtain robust velocity estimation, we need seismic inversion. The estimated preliminary Vp and Vs profiles as well as densities obtained from regional data are used as an initial model for waveform modeling and inversion for Vp from streamer data. We use a two-step procedure method for least-squares and conjugate gradient algorithm developed by Wang et al. (2002) to solve this nonlinear inversion problem.

Examples

Both OBS hydrophone and MCS data from the Oregon seismic experiment demonstrate a strong BSR indicating the presence of gas hydrate above and free gas below. Many reflections can be reliably correlated between the two data sets.

The interactive V_p and V_s analysis of the OBS data in τ-p domain allow identification of two types of converted-waves (Rps and Rpss) and a conversion surface, separating a layer with low P-wave velocity overlying a layer with high P-wave velocity. An incident P-wave converts into a transmitted S-wave at this interface. Similar structures of Vp, Vs and Poisson's ratio can be observed among different OBS locations. The estimated Vp and Vs profiles, as well as density profile from the regional data, can be used as initial model for waveform inversion.

Since the OBS data were recorded only at some sparse spatial locations, we used large offset streamer data in the inversion. Due to its close proximity to OBS 102ns, we first inverted CMP 1820 followed by several CMP gathers along the Line 103. We applied pre-stack (multi-offset) waveform inversion for Vp, impedance, and Poisson's ratio with an assumption that the medium is isotropic and is described solely by Vp, Vs and density. The inverted Vp profile of CMP 1820 (Fig. 2) has a low velocity layer existing below the sea floor, which is different from the conventional Vp gradients involving gas hydrates. This lower velocity layer exists under the summit area from CMP 1820 to CMP 2200 sites along Line 103.

To explain velocity profiles, we need to relate the basic feature in the inverted Vp profile to the observation of Suess et al. (2001). In the Hydrate Ridge area gas

hydrates were also exposed on the seafloor and two types of hydrate fabrics, massive and porous hydrates, were clearly observed by submersible and deep-towed video survey (Suess et al., 2001). The inverted (from seismic data) Vp profiles can be interpreted by identifying the two types of hydrate fabrics. Fig. 2 shows three major zones identified on the inverted Vp profile derived from CMP 1982. The model shows a high velocity hydrate layer sandwiched between two low velocity layers. The low P-wave velocity (about 1.25-1.5 km/s) immediately below the sea floor may be interpreted as a seismic response from a zone of porous hydrate. The size of pores, as well as the porosity, within the porous hydrate layer gradually decreases downward leading to a positive velocity gradient. High P-wave velocity (1.63-1.72 km/s) below the conversion surface indicates normal massive (non-porous) gas hydrate. The low Vp (1.47-1.62 km/s) layer below this (i.e., below BSR) shows the presence of free gas in the sediment pores. The layer below the free gas zone is likely to be the normal liquid-saturated sedimentary section. The inverted Vp profile suggests that normal gas hydrate occurs at depths of about 65 m below the seafloor. Recent drilling (July 2002) at the southern summit of Hydrate Ridge has confirmed the presence of normal massive gas hydrate at depth that the Vp inversion results suggested. Free gas was encountered below normal massive gas hydrate.

The lateral variations of the identified porous hydrate, massive hydrate and free gas are well defined by the velocity profiles derived from the selected CMP gathers (1780 through 2440) along the Line 103 (Fig. 3). Around the ridge, the porous hydrate forms a thicker layer, but it gradually disappears toward land (toward east in the figure) into the slope basin, and disappears seaward from CMP 1800 where a large fault exists. Correspondingly, the normal massive hydrate is not thick, and gradually thickens eastward toward land into the slope basin. Free gas forms a continuous zone below the BSR, and is very thick in the slope basin. A series of faults serve as conduits of ascending fluids and the generous supply of gas controls the distribution of porous hydrate. Free gas rises along the faults to the shallow zone, and spreads laterally to form a steady porous hydrate zone around the ridge where faults are well developed. Both acoustic impedance and Poisson's ratio profiles demonstrated a similar distribution and variation of the porous hydrate, massive hydrate and free gas layers as in the Vp-section.

Comprehensive genetic interpretation of gas hydrates is summarized in Fig. 4. According to the fluid expulsion model for gas hydrate formation developed by Hyndman and Davis (1992), hydrate layers are formed mainly through the removal of methane from upward moving pore fluids as they pass into the hydrate stability field. Fig. 4(a**)** is a sketch of accretionary complex showing the methane production, methane removal from upward moving pore fluids, and methane hydrate formation. Original methane is mainly generated in basin sediments, and is migrated to the shallow zone in the accretionary compex to form gas hydrates by an equilibrium porosity-depth relation through consolidation and fluid expulsion. At the southern summit of Hydrate Ridge, the faults related to the evolution and growth of the accretionary complex of Cascadia convergent margin provide the pathways for methane and fluid venting, which have influence on final gas hydrate distribution (Fig. 4b). The faults extend through the accreted sediments to below the gas hydrate phase transition. At depth, they tap a fluid reservoir containing free methane. The faults serve as conduits and channel methane up to the near-seafloor where it forms secondary gas hydrates with bubble fabric, or up to the seafloor where it either escapes into the water column or forms secondary gas hydrates with massive fabric. Therefore, thin (less than 0.5 m) massive hydrate, porous hydrate, normal massive hydrate and free gas distribute from the seafloor to below BSR. Suess et al. (2001) summarized development of bubble fabric and evolution of seafloor hydrate layers at the southern summit (Fig. 4c). Hydrate with porous fabric develops from the accumulation of methane bubbles as they become encased in a hydrate skin. Bubbles, rising from the below the seafloor, either escape into the water column or when arrested, turns into hydrate. The porous hydrate fabric consists of macroscopic pores, which are connected by thin veneer of hydrate. Growth of a hydrate skin impedes further reaction between bubble and water. At the seafloor they may form positively buoyant interlayered strata including hydrate, sediments, carbonate, microbial mats, free gas and water.

Conclusions

The combination of OBS and streamer MCS data allows us to identify the presence of gas hydrate, detect the distribution gas hydrate and interpret the formation of gas hydrate at the Hydrate Ridge offshore Oregon.

References

Hyndman, R.D., and Davis, E.E., 1992, A mechanism for the formation of methane hydrate and seafloor bottom simulating reflectors by vertical fluid expusion, Journal of Geophysical Research, v. 97(B5), 7025-7041.

Hyndman, R.D., and Spence, G.D., 1992, A seismic study of methane hydrate marine bottom simulating reflectors: Journal of Gephysical Research, 97(B5), 6683-6698.

Kvenvolden, K.A., 1993, Methane hydrates—Geological perspective and global change, Review of Geophysics, v. 31, p. 173-187.

Sloan, E.D., Jr., 1990, Clathrate hydrates of natural gases: Marcel Dekker, 641p.

Sloan, E.D., Jr., 1998, Clathrate hydrates of natural gases, 2nd ed.: Marcel Dekker, 705p.

Suess, E., Torres, M.E., Bohrmann, G., Collier, R.W., Rickert, D., Goldfinger, C., Linke, P., Heuser, A., Sahling, H., Heeschen, K., Jung, C., Nakamura, K., Greinert, J., Pfannkuche, O., Trehu, A., Klinkhammer, G., Whiticar, M.J., Eisenhauer, A., Teichert, B., and Elvert, M., 2001, Sea floor methane hydrates at Hydrate Ridge, Cascadia Margin, In: C.K. Paul, and W.P. Dillon, eds., Natural Gas Hydrates: Occurrence, Distribution, and Detection, Geophysical Monograph 124, pp. 87-98.

Wang, C, Sen, M., and McIntosh, K., 2002, Velocity Estimation from post-stack seismic data and density log by a linearized Inversion, SEG Extended Abstract xxx

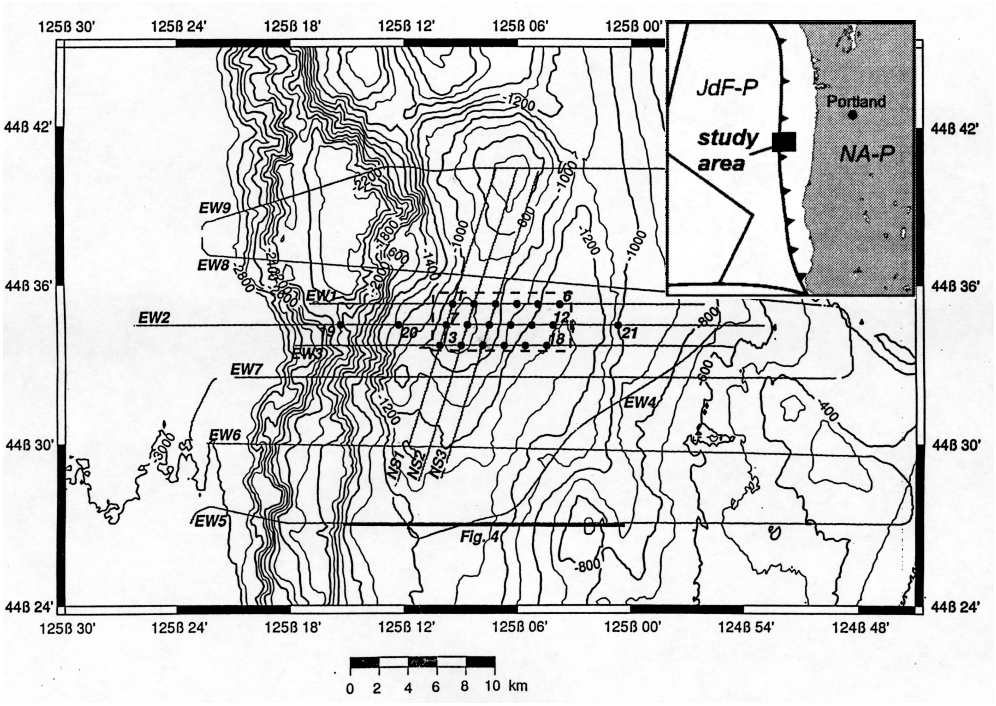

Fig. 1. Bathymetric map showing regional lines, OBS locations (numbered dots), and the location of the 3D seismic survey (dashed box). Inset shows regional tectonic setting and location of study area.

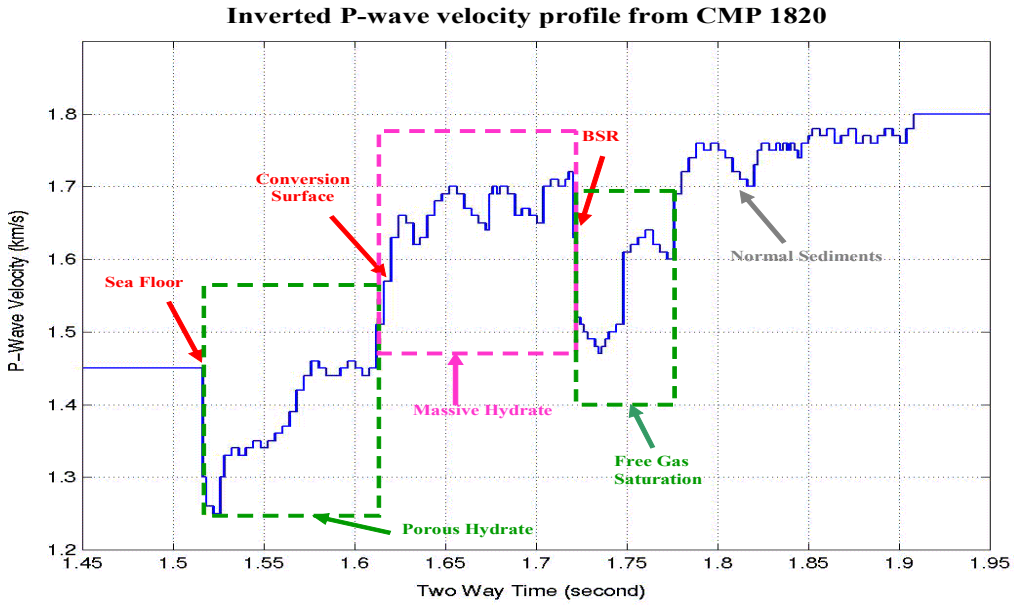

Fig. 5. Interpretation of the inverted P-wave velocity profile. Four major layers are identified. Layer 1: Porous hydrate with low P-wave velocity; Layer 2: Normal massive gas hydrate with high P-wave velocity; and Layer 3: Free gas saturation with low P-wave velocity.

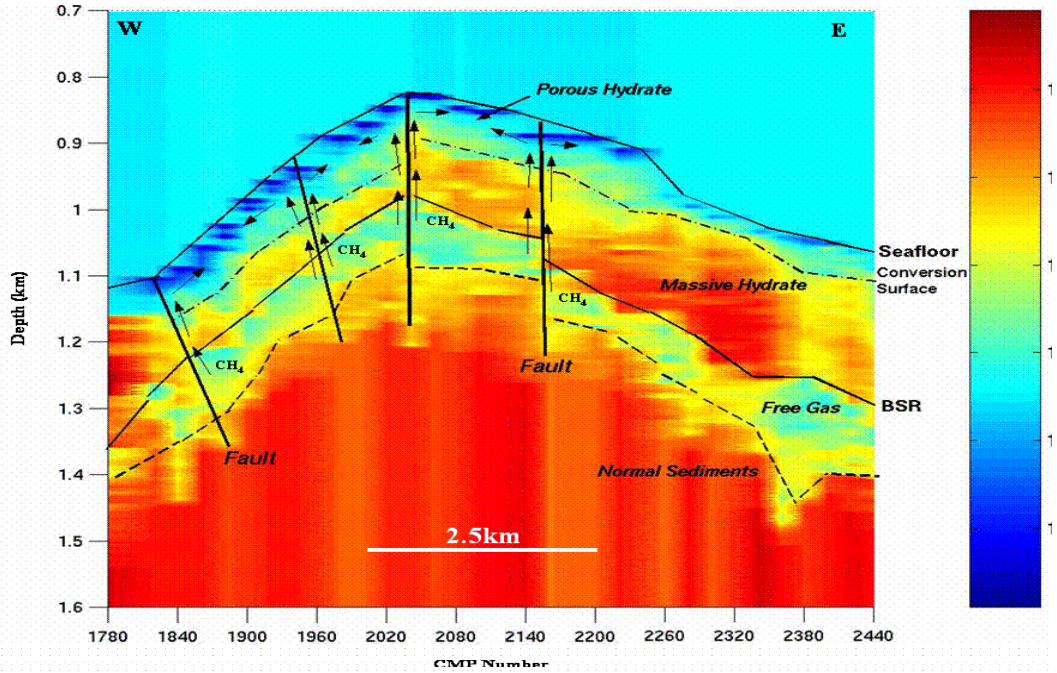

Fig. 3. The velocity profiles derived from inversion along the Line 103 across the Hydrate Ridge. Three basic velocity layers are identified below sea floor: Layer 1 — lower velocity, representing porous hydrate; Layer 2 — high velocity, reflecting massive hydrate; Layer 3 — lower velocity, indicating free gas.

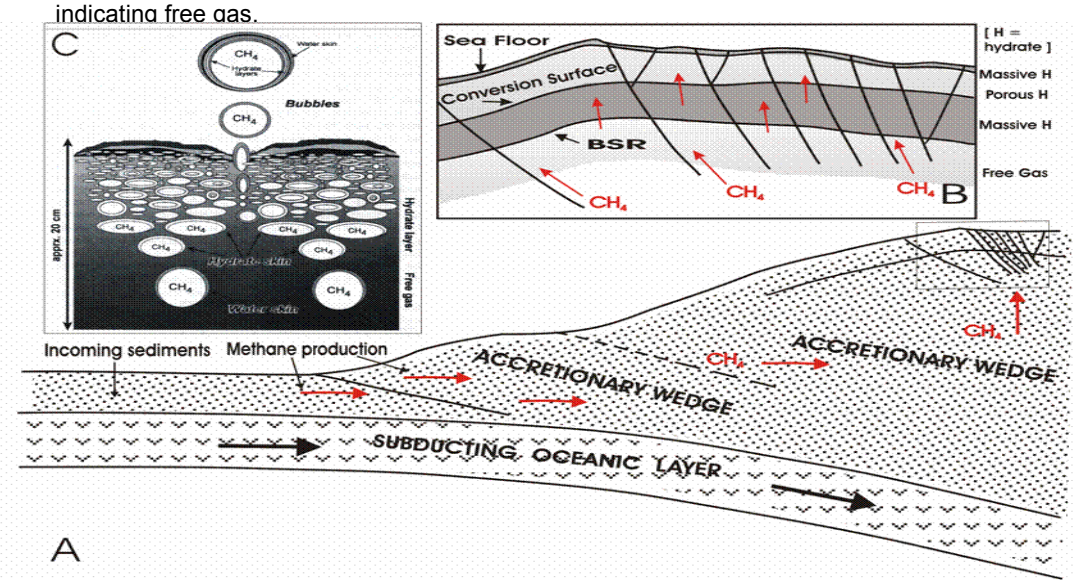

Fig. 4. Geological interpretation. A – Sketch of accretionary complex showing production and migration of methane; B – distribution of gas hydrates and free gas at the southern summit of the Hydrate Ridge, two types of gas hydrates: massive hydrate with high velocity, and porous hydrate with low velocity; C – development of bubble fabric and evolution of seafloor hydrate layers (from Suess et al., 2001).